ISSN: 2277-9655
(I2OR), Publication Impact Factor: 3.785

IJESRT

INTERNATIONAL JOURNAL OF ENGINEERING SCIENCES & RESEARCH TECHNOLOGY

MHD MIXED CONVECTION FLOW OF A MICROPOLAR FLUID OVER AN UNSTEADY STRETCHING SURFACE WITH VISCOUS DISSIPATION AND HEAT SOURCE/SINK

Dr.M.Sreedhar Babu*, M.Lavanya, G.Venkata Ramanaiah
Asst.professor, Dept. of Applied Mathematics, Y.V.University, Kadapa Andhra Pradesh, India.
Research scholar, Dept. of Applied Mathematics, Y.V.University, Kadapa Andhra Pradesh, India.
Research scholar, Dept. of Applied Mathematics, Y.V.University, Kadapa Andhra Pradesh, India.

ABSTRACT

The unsteady, two dimensional, mixed convection flow of an viscous incompressible electrically conducting micropolar fluid over a vertical and impermeable stretching surface in the presence of Magnetic field, Heat source/sink and mass transfer when the buoyancy force assists os opposes the flow has been studied. Using the similarity transformations, the governing equations have been transformed into a system of ordinary differential equations. These differential equations are highly nonlinear which cannot be solved analytically. Therefore, fourth order Runge-Kutta method along with shooting technique has been used for solving it. Numerical results are obtained for the skin-friction coefficient, the couple wall stress, the local Nusselt number and Sherwood number as well as the velocity, microrotation, temperature and concentration profiles for different values of the governing parameters, namely, material parameter, magnetic parameter, unsteadiness parameter, heat source/sink parameter, Eckert number and Schmidt number.

KEYWORDS: unsteady flow, mixed convection, heat and mass transfer, micropolar fluid, MHD, stretching surface, heat source or sink, viscous dissipation.

INTRODUCTION

The theory of micropolar fluids has received great attention during the recent years, because the traditional Newtonian fluids cannot precisely describe the characteristic of fluid with suspended particles. A micropolar fluid obeys the constitutive equations of the considered non-Newtonian fluid model. In the micropolar fluid model, apart from the classical velocity field, a microrotation vector and a gyration parameter are introduced in order to investigate the kinematics of microrotation. Such fluid model may be applied to explain the flow of colloidal solutions, liquid crystals, fluids with additives, suspension solutions, animal blood, etc. The presence of dust or smoke particular in a gas may also be modelled using micropolar fluid dynamics. Unlike the other fluids, micropolar fluids are fluids with microstructure belonging to a class of fluids with non-symmetrical stress tensor. Physically, they represent fluids consisting of randomly oriented particles suspended in a viscous medium. The theory of micropolar fluids, first proposed by Eringen [1, 2] is capable of describing such fluids. In this theory the local effects arising from the microstructure and the intrinsic motion of the fluid elements are taken into account. This is a kind of continuum mechanics, and many classical flows are being re-examined to determine the effects of fluid microstructure [3-5]. Early studies along these lines may be found in the review article by Peddieson and McNitt [6], and in the recent books by Lukaszewicz [7] and Eringen [8]. The boundary layer flow and heat transfer in a quiescent Newtonian and non- Newtonian fluid driven by a continuous stretching sheet is of significance in a number of industrial engineering processes, such as the drawing of a polymer sheet or filaments extruded continuously from a die, the cooling of a metallic plate in a bath, the aerodynamic extrusion of plastic sheets, the continuous casting, rolling, annealing and tinning of copper wires, the wire and fiber coating, etc. During the processes, mechanical properties are greatly dependent upon the rate of cooling.

The free convection effect on MHD coupled heat and mass transfer of a moving vertical surface has been studied by Yih [9]. Anjali Devi and Kandasamy [10] studied the steady MHD laminar boundary layer flow over a wall of the wedge with suction and injection in the presence of species concentration and by considering the mass diffusion. The effects of Dufour and Soret numbers on unsteady MHD free convection and mass transfer flow past an infinite vertical

porous plate embedded in a porous medium have been considered by Alam et al. [11]. Xu and Liao [12] examined the unsteady MHD flows of a non-Newtonian fluid over a nonimpulsively stretching flat sheet and presented an accurate series solution. Abdelkhalek [13] investigated the free convection from a moving vertical surface in a MHD flow using perturbation technique. MHD effects on impulsively started vertical infinite plate with variable temperature in the presence of transverse magnetic field were studied by Soundalgekar et al. [14]. Hasanpour et al. [15] investigated the MHD mixed convective flow in a lid-driven cavity filled with porous medium using numerical method. They concluded that the fluid circulations within the cavity are reduced by increasing magnetic field strength as well as Darcy number reduction. Kumar and Verma [16] studied the problem of an unsteady flow past an infinite vertical permeable plate with constant suction and transverse magnetic field with oscillating plate temperature. Recently, Hasanpour et al. [17] studied the investigation of heat and mass transfer of MHD flow over the movable permeable plumb surface using HAM

The heat source/sink effects in thermal convection, are significant where there may exist a high temperature difference between the surface (e.g. space craft body) and the ambient fluid. Heat generation is also important in the context of exothermic or endothermic chemical reactions. Postelnicu et al. [18] investigated the effect of variable viscosity on forced convection over a horizontal flat plate in a porous medium with internal heat generation. Molla et al. [19] studied natural convection flow along a vertical wavy surface with uniform surface temperature in presence of heat generation/absorption. MHD heat and mass transfer free convection flow along a vertical stretching sheet in presence of magnetic field with heat generation are studied by Samad et al. [20]. Bhaskar Reddy and Bathaiah [21] analyzes the hydrodynamic channel flows under periodic rate of heat generation with Hall effects. Alam et al [22] analyzed the study of the combined free - forced convection and mass transfer flow past a vertical porous plate in a porous medium with heat generation and thermal diffusion. Recently, Rahman et al. [23] investigated the thermophoresis effect on MHD forced convection on a fluid over a continuous linear stretching sheet in presence of heat generation and Power-Law wall temperature

Unsteady free convection flows of dissipative fluids past an infinite plate have received a little attention because of non-linearity of the governing equations. Gebhart [24] has shown the importance of viscous dissipative heat in free convection flow in the case of isothermal and constant heat flux at the plate. Gebhart and Mollendorf [25] considered the effects of viscous dissipation for external natural convection flow over a surface. Neeraja and Bhaskar Reddy [26] investigated the MHD unsteady free convection flow past a vertical porous plate with viscous dissipation. Recently, Abd El-Aziz [27] studied the mixed convection flow of a micropolar fluid from an unsteady stretching surface with viscous dissipation.

The present study investigates an unsteady mixed convection flow of a viscous incompressible electrically conducting micropolar fluid on a vertical and impermeable stretching sheet in the presence of transverse magnetic field and heat generation or absorption. Using the similarity transformations, the governing equations have been transformed into a set of ordinary differential equations, which are nonlinear and cannot be solved analytically, therefore, fourth order Runge-Kutta method along with shooting technique has been used for solving it. The numerical results for the velocity, microrotation, temperature and concentration functions are carried out for a wide range of important parameters namely, material parameter, magnetic parameter, Eckert number, unsteadiness parameter, heat source/sink parameter and Schmidt number. The skin friction, the couple wall stress, the rate of heat transfer and the rate of mass transfer have also been computed.

MATHEMATICAL FORMULATION

Consider an unsteady two dimensional, mixed convection boundary layer flow of a viscous incompressible micropolar fluid over an elastic, vertical and impermeable stretching sheet which emerges vertically in the upward direction from a narrow slot with velocity [28]

$$U_w(x,t) = \frac{ax}{1-\alpha t} \tag{2.1}$$

where both a and α are positive constants with dimension per time.

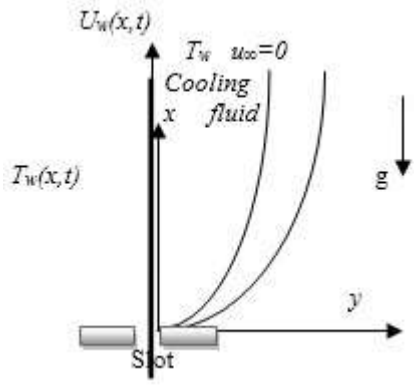

Figure A: Schematic representation of the physical model and coordinate system

A schematic representation of the physical model and coordinates system is depicted in Figure A. The positive *x* coordinate is measured along the stretching sheet with the slot as the origin and the positive *y* coordinate is measured normal to the sheet in the outward direction toward the fluid. The surface temperature T_w and concentration C_w of the stretching sheet varies with the distance x from the slot and time t as

$$T_w(x,t)=T_\infty+\frac{bx}{(1-\alpha t)^2},C_w(x,t)=C_\infty+\frac{cx}{(1-\alpha t)^2} \qquad (2.2)$$

where *b* and *c* are constants with dimension temperature and concentration over length and υ is the kinematic viscosity of the ambient fluid. It is apt to note here that, the expressions for $U_w(x, t)$ and $T_w(x, t)$ in equations. (2.1) and (2.2) are valid only for time $t=\alpha^{-1}$ unless $\alpha=0$. Expression (2.1) for the velocity of the sheet $U_w(x, t)$ reflects that the elastic sheet which is fixed at the origin is stretched by applying a force in the positive x -direction and the effective stretching rate $\frac{a}{(1-\alpha t)}$ increases with time. With the same analogy the expression for the surface temperature $T_w(x, t)$ and $C_w(x, t)$ given by equation (2.2) represents a situation in which the sheet temperature increases (reduces) if b, c are positive (negative) from T_∞, C_∞ at the slot in proportion to *x* and such that the amount of temperature and concentration increase (reduction) along the sheet increases with time. A uniform magnetic field of strength B_0 is assumed to be applied in the positive y-direction normal to the plate. The magnetic Reynolds number of the flow is taken to be small enough so that the induced magnetic field is negligible. It is further assumed that the fluid properties are taken to be constant except for the density variation with the temperature and concentration in the buoyancy terms (Boussinesq approximation). Under the usual boundary layer approximation, the governing equations are

Continuity equation

$$\frac{\partial u}{\partial x}+\frac{\partial v}{\partial y}=0 \qquad (2.3)$$

Linear momentum equation

$$\frac{\partial u}{\partial t}+u\frac{\partial u}{\partial x}+v\frac{\partial u}{\partial y}=\left(\frac{\mu+\kappa}{\rho}\right)\frac{\partial^2 u}{\partial y^2}-\frac{\sigma B_0^2}{\rho}u+\frac{\kappa}{\rho}\frac{\partial N}{\partial y}+g\beta_T\left(T-T_\infty\right)+g\beta_C\left(C-C_\infty\right) \qquad (2.4)$$

Angular momentum equation

$$\rho j\left(\frac{\partial N}{\partial t}+u\frac{\partial N}{\partial x}+v\frac{\partial N}{\partial y}\right)=\gamma\frac{\partial^2 N}{\partial y^2}-\kappa\left(2N+\frac{\partial u}{\partial y}\right) \qquad (2.5)$$

Energy equation

$$\frac{\partial T}{\partial t}+u\frac{\partial T}{\partial x}+v\frac{\partial T}{\partial y}=\alpha\frac{\partial^2 T}{\partial y^2}+\left(\frac{\mu+\kappa}{\rho c_p}\right)\left(\frac{\partial u}{\partial y}\right)^2+q(T-T_\infty) \tag{2.6}$$

Species equation

$$\frac{\partial C}{\partial t}+u\frac{\partial C}{\partial x}+v\frac{\partial C}{\partial y}=D\frac{\partial^2 C}{\partial y^2} \tag{2.7}$$

The boundary conditions for the velocity, temperature and concentration fields are

$$\begin{aligned} &u=U_w, v=0, N=0, T=T_w, C=C_w \quad \text{at} \quad y=0 \\ &u\to 0, N\to 0, T\to T_\infty, C\to C_\infty \quad \text{as} \quad y\to\infty \end{aligned} \tag{2.8}$$

where *u* and *v* are the velocity components in the *x* - and *y* - directions, respectively, *T* is the fluid temperature in the boundary layer, *C* is the fluid temperature in the boundary layer, *N* is the component of the microrotation vector normal to the x-y plane, σ is the spin-gradient viscosity, $\alpha_0 (= k/\rho c_p)$ is the thermal diffusivity and k is the fluid thermal conductivity, c_p is the heat capacity pressure, respectively.

The continuity equation (2.3) is satisfied by the Cauchy Riemann equations

$$u=\frac{\partial \psi}{\partial y} \quad \text{and} \quad v=-\frac{\partial \psi}{\partial x} \tag{2.9}$$

where $\psi(x,y)$ is the stream function.

In order to transform the equations (2.4), (2.5) (2.6), (2.7) and (2.8) into a set of ordinary differential equations, the following similarity transformations and dimensionless variables are introduced.

$$\begin{aligned} &\eta=\sqrt{\frac{a}{\upsilon(1-\alpha t)}}y, \psi=\sqrt{\frac{\upsilon a}{1-\alpha t}}xf(\eta), N=\sqrt{\frac{a^3}{\upsilon(1-\alpha t)^3}}xh(\eta) \\ &T=T_\infty+\frac{bx}{(1-\alpha t)^2}\theta(\eta), C=C_\infty+\frac{cx}{(1-\alpha t)^2}\phi(\eta), A=\frac{\alpha}{a}, K=\frac{\kappa}{\mu} \\ &M=\frac{\sigma B_0^2}{\rho a}, \Pr=\frac{\upsilon}{\alpha_0}, Sc=\frac{\upsilon}{D}, Gr_x=\frac{g\beta_T(T_w-T_\infty)x^3}{\upsilon^2}, \mathrm{Re}_x=\frac{U_w x}{\upsilon} \\ &Gc_x=\frac{g\beta_C(C_w-C_\infty)x^3}{\upsilon^2}, \lambda_0=\frac{\gamma}{\mu j}, \lambda=\frac{g\beta_T b}{a^2}=\frac{Gr_x}{\mathrm{Re}_x^2}, \delta=\frac{g\beta_C c}{a^2}=\frac{Gc_x}{\mathrm{Re}_x^2} \\ &B=\frac{\upsilon(1-\alpha t)}{jb}=\frac{\upsilon x}{jU_w}, Ec=\frac{U_w^2}{c_p(T_w-T_\infty)}, Q=\frac{q}{\rho c_p a} \end{aligned} \tag{2.10}$$

where $f(\eta)$ is the dimensionless stream function, θ is the dimensionless temperature, ϕ is the dimensionless concentration, η is the similarity variable, *A* is the unsteadiness parameter, M is the magnetic parameter, *Ec* is the Eckert number, *Q* is the heat source/sink parameter, Gr_x is the thermal Grashof number, Gc_x is the solutal Grashof number, λ is the thermal buoyancy parameter, δ is the solutal buoyancy parameter, λ_0, B are the dimentionless

parameters, Re_x is the local Reynolds number, *Pr* is the Prandtl number, and Sc is the Schmidt number.

In view of the equations (2.9) and (2.10), the equations (2.4), (2.5), (2.6), (2.7) and (2.8) transform into

$$(1+K)f''' + ff'' - (f')^2 + Kh' - Mf' - \frac{A}{2}(2f' + \eta f'') + \lambda\theta + \delta\phi = 0 \quad (2.11)$$

$$\lambda_0 h'' + fh' - f'h - KB(2h + f'') - \frac{A}{2}(3h + \eta h') = 0 \quad (2.12)$$

$$\frac{1}{\mathrm{Pr}}\theta'' + f\theta' - f'\theta - \frac{A}{2}(4\theta + \eta\theta') + Q\theta + Ec(1+K)(f'')^2 = 0 \quad (2.13)$$

$$\frac{1}{Sc}\phi'' + f\phi' - f'\phi - \frac{A}{2}(4\phi + \eta\phi') = 0 \quad (2.14)$$

The corresponding boundary conditions are

$$f = 0,\ f' = 1,\ h = 0,\ \theta = 1,\ \phi = 1 \quad \text{at} \quad \eta = 0$$
$$f' = h = \theta = \phi = 0 \quad \text{as} \quad \eta \to \infty \quad (2.15)$$

where the primes denote differentiation with respect to η

for the type of the problem under consideration, the physical quantities of interest are the skin friction coefficient C_{fx}, the local couple wall stress M_{wx}, the local Nusselt number Nu_x and Sherwood number Sh_x which are defined as

$$C_{fx} = \frac{2}{\rho U_w^2}\left[(\mu + \kappa)\left(\frac{\partial u}{\partial y}\right)_{y=0} + \kappa(N)_{y=0}\right] = 2(1+K)\mathrm{Re}_x^{-1/2} f''(0) \quad (2.16)$$

$$M_{wx} = \gamma\left(\frac{\partial N}{\partial y}\right)_{y=0} = \frac{\gamma a U_w}{\upsilon(1-\alpha t)} h'(0) \quad (2.17)$$

$$Nu_x = -\frac{x}{T_w - T_\infty}\left(\frac{\partial T}{\partial y}\right)_{y=0} = -\mathrm{Re}_x^2\,\theta'(0) \quad (2.18)$$

$$Sh_x = -\frac{x}{C_w - C_\infty}\left(\frac{\partial C}{\partial y}\right)_{y=0} = -\mathrm{Re}_x^2\,\phi'(0) \quad (2.19)$$

Our main aim is to investigate how the values of $f''(0)$, $h'(0)$, $-\theta'(0)$ and $-\phi'(0)$ vary in terms of the various parameters.

SOLUTION OF THE PROBLEM

The set of coupled non-linear governing boundary layer equations (2.11) - (2.14) together with the boundary conditions (2.15) are solved numerically by using Runge-Kutta fourth order technique along with shooting method. First of all, higher order non-linear differential equations (2.11) - (2.14) are converted into simultaneous linear differential equations of first order and they are further transformed into initial value problem by applying the shooting technique (Jain *et al.*[29]). The resultant initial value problem is solved by employing Runge-Kutta fourth order technique. The step size $\Delta\eta$=0.05 is used to obtain the numerical solution with five decimal place accuracy as the criterion of convergence. From the process of numerical computation, the skin-friction coefficient, the Nusselt number and the Sherwood number, which are respectively proportional to $f''(0), -\theta'(0)$ and $-\phi'(0)$, are also sorted out and their numerical values are presented in a tabular form.

RESULTS AND DISCUSSION

The governing equations (2.11) - (2.14) subject to the boundary conditions (2.15) are integrated as described in section 3. In order to get a clear insight of the physical problem, the velocity, angular velocity, temperature and concentration have been discussed by assigning numerical values to the parameters encountered in the problem.

Physically $\lambda, \delta > 0$ means heating of the fluid or cooling of the surface (assisting flow), $\lambda, \delta < 0$ means cooling of the fluid or heating of the surface (opposing flow) and $\lambda, \delta = 0$ means the absence of free convection currents (forced convection flow). Figs. 1-4 illustrate the axial velocity, angular velocity, temperature and concentration fields for different values of the magnetic parameter (M). It is observed that for both (assisting flow) and (opposing flow) that the axial velocity $f'(\eta)$ and angular velocity $h(\eta)$ decrease while the temperature $\theta(\eta)$ and concentration $\phi(\eta)$ increases with an increase in the magnetic parameter. The magnetic parameter is found to retard the velocity at all points of the flow field. It is because that the application of transverse magnetic field will result in a resistive type force (Lorentz force) similar to drag force which tends to resist the fluid flow and thus reducing its velocity.

Representative axial velocity, angular velocity, temperature and concentration profiles in the case of assisting and opposing flows and for various values of the micropolar parameter *K* are presented in Figs. 5-8. It is found that for both (assisting flow) and (opposing flow) that the axial velocity $f'(\eta)$ and angular velocity $h(\eta)$ increase while the temperature $\theta(\eta)$ and concentration $\phi(\eta)$ decreases with an increase in the micropolar parameter K but the effect of K on the velocity, temperature and concentration fields is more pronounced in the case of opposing flow. When $K = 0$ (Newtonian fluid) there is no angular velocity, and as K increases, the angular velocity is greatly induced. Further, the micropolar parameter K demonstrates a more pronounced influence on the axial and angular velocities $f'(\eta)$ and $h(\eta)$ respectively, than that on the temperature $\theta(\eta)$ and concentration $\phi(\eta)$. Moreover, it is seen from Figs. 5 and 6 that the smaller the K, the thinner the momentum and angular momentum boundary layer thickness while the opposite trend is true for the thermal and concentration boundary layer as obvious from Figs. 7 and 8.

Representative axial velocity, angular velocity, temperature and concentration profiles in the case of assisting and opposing flows and various values of the heat source/sink parameter *Q* are presented in Figs. 9-12. It is found that for both positive (assisting flow) and negative (opposing flow) λ, δ that the axial velocity $f'(\eta)$ and angular velocity $h(\eta)$ increase in case of assisting flow where as decrease in case of opposing flow while the concentration $\phi(\eta)$ decreases in case of assisting flow whereas increase in case of opposing flow with an increase in the heat source/sink parameter but the effect of Q on the temperature $\theta(\eta)$ increases in both the assisting and opposing flows with an increase in the heat source/sink parameter.

Figs. 13-16 shows the profiles of the velocity, angular velocity, temperature and concentration distribution against η for various values of Eckert number *Ec* in the case of assisting and opposing flows. It is known that the viscous dissipation produces heat due to drag between the fluid particles and this extra heat causes an increase of the initial fluid temperature (see Fig.15). This increase of temperature causes an increase of the buoyant force. Also, there is a continuous interaction between the viscous heating and the buoyant force. This mechanism produces different results in the assisting (upward) and opposing (downward) flow. In the assisting (opposing) flow, the increase in the values of positive (negative) Ec will increase the buoyant force in the upward (downward) direction which results in an increase in the fluid velocity as shown in Fig. 13. The positive (Ec > 0) and negative (Ec < 0) Eckert numbers assists the upward ($\lambda,\delta > 0$ and hence Ec >0) and downward ($\lambda,\delta < 0$ and hence Ec < 0) flow, respectively as shown in Fig. 13. It is noted from Fig. 14 that the angular velocity $h(\eta)$ first decreases near the stretching surface where

$0 \le \eta < \eta_0$ where $\eta_0 \cong 1.4$ in the case of assisting flow and $\eta \cong 1.6$ in the case of opposing flow but the situation is completely reversed in the other part of the boundary layer where $\eta > \eta_0$. It is observed from Fig.16 that the concentration decrease with an increase in the Eckert number.

According to the definition of Eckert number, a positive Ec corresponds to fluid heating (heat is being supplied across the walls into the fluid) case ($T_w > T_\infty$) so that the fluid is being heated whereas a negative Ec means that the fluid is being cooled. From Fig. 15 it is seen that the dimensionless temperature increases when the fluid is being heated (Ec >0) but decrease when the fluid is being cooled (Ec < 0). For Ec < 0 the dimensionless fluid temperature $T_w < T_\infty$ decreases monotonically with η, from unity at the wall towards its free-stream value. It is noted from the definition of θ that this behavior implies the monotonous decrease in the actual fluid temperature in the horizontal direction from the sheet temperature T_w to the free-stream temperature. On the other hand, for Ec < 0 (i.e. $T_w < T_\infty$) the dimensionless fluid temperature θ decreases with η rapidly at first, arriving at a negative minimum value, for Ec = -4 and then increases more gradually to its free surface value. Correspondingly, the actual fluid temperature in the horizontal direction increases at first from the surface temperature T_w to a maximum value and then decrease to its free-stream value. It should be noted that for the fluid cooling case (Ec < 0) a negative θ indicates the excess of actual fluid temperature T over that at the plate because of the viscous dissipation effect.

Fig. 17-20 shows the variation of the skin friction, couple wall stress, Nusselt number and Sherwood number with for different values of magnetic parameter and unsteadiness parameter (*A*). It is observed that the skin friction increases with an increase in the *M* or *A*, and couple wall stress increases with increasing the *M* or *A*. It is observed that the heat and mass transfer rates increases with an increase in the parameter A and decreases with increasing the parameter *M*. Fig. 21-24 depicts the variation of the skin friction, couple wall stress, Nusselt number and Sherwood number with for different values of unsteadiness parameter and material parameter. It is noticed that the skin friction decreases with an increase in the parameter *A* and increases with increasing the material parameter. It is observed that the couple wall stress, Nusselt number and Sherwood number increases with an increase in the parameters *A* or *K*.

Variations of the local skin friction coefficient, the wall couple stress, the local Nusselt number and the local Sherwood number as a function of the unsteadiness parameter *A* for various values of Eckert number are presented in Figs. 25-28. It is clear from Fig. 25 that for fixed *A* the skin friction coefficient increases as *Ec* increases for both opposing and assisting flow cases. In addition, the effect of viscous dissipation on is more pronounced for lower values of *A*. It is also observed that the local skin friction coefficient of buoyancy assisting flow is higher than that of buoyancy opposing flow for all values of *A* and *Ec*. The effect of viscous dissipation on the wall couple stress is completely opposite to that on the local skin friction coefficient as obvious from Fig. 26. Further, viscous dissipation demonstrates a more pronounced influence on the wall couple stress in the opposing flow than that of assisting flow. For given Fig. 27 demonstrates that the heat transfer rate is enhanced for fluid cooling case (*Ec* < 0 and λ, δ < 0) but it is reduced for the fluid heating case (*Ec* > 0 and λ, δ >0). These behaviours are consistent with the results of the dimensionless temperature profiles shown in Fig. 15, where the wall temperature gradient is increased for *Ec* < 0 but is decreased for *Ec* > 0. Also, the influence of viscous dissipation on the heat transfer is seen to be more noticeable for higher values of the unsteadiness parameter *A*. In addition, the local heat transfer coefficient takes a higher value for a negative Eckert number *Ec* but a lower value for a positive *Ec*, as compared with the case of no viscous dissipation (*Ec* = 0). Fig. 28 demonstrates that the mass transfer rate is reduced for fluid cooling case (*Ec* < 0 and λ, δ < 0) but it is enhanced for the fluid heating case (*Ec* > 0 and λ, δ >0). These behaviors are consistent with the results of the dimensionless concentration profiles shown in Fig. 16, where the wall concentration gradient is decreased for *Ec* < 0 but is increased for Ec > 0. In addition, the local mass transfer coefficient takes a lower value for a negative Eckert number *Ec* but a higher value for a positive *Ec*, as compared with the case of no viscous dissipation (*Ec* = 0).

For validation of the numerical method used in this study, results for $-\theta'(0)$, were compared with those of Ishak et al. [30] for various values of *A, λ* and *Pr*. The quantitative comparison is shown in **Table 1** and it is found to be in excellent agreement.

CONCLUSIONS

In the present prater, the unsteady mixed convection flow of an viscous incompressible electrically conducting micropolar fluid on a vertical and impermeable stretching surface with heat generation or absorption by taking mass transfer into account, are analyzed. The governing equations are approximated to a system of non-linear ordinary differential equations by similarity transformation. Numerical calculations are carried out for various values of the dimensionless parameters of the problem. It has been found that

1. The velocity decreases as well as the angular velocity, temperature and concentration increases with an increase in the magnetic parameter in both assisting and opposing flows.
2. The velocity and angular velocity increases as well as the temperature and concentration decreases with an increase in the material parameter in both assisting and opposing flows.
3. The heat source/sink and viscous dissipation enhances the velocity, angular velocity and temperature, and reduces the concentration in both assisting and opposing flows.
4. The skin friction reduces the magnetic parameter or unsteadiness parameter and increases the material parameter in both assisting and opposing flows.
5. The unsteadiness parameter enhances the couple wall stress, heat and mass transfer rates.

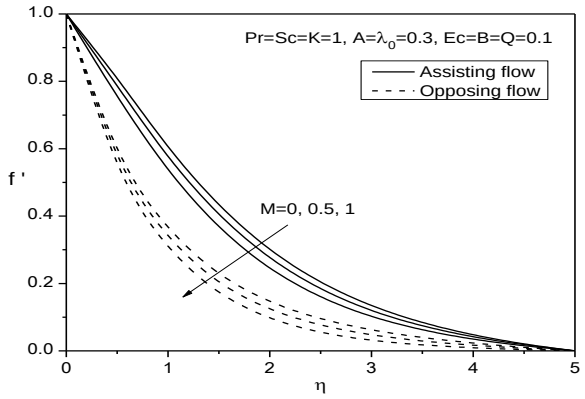

Fig.1 Velocity profiles for different values of M

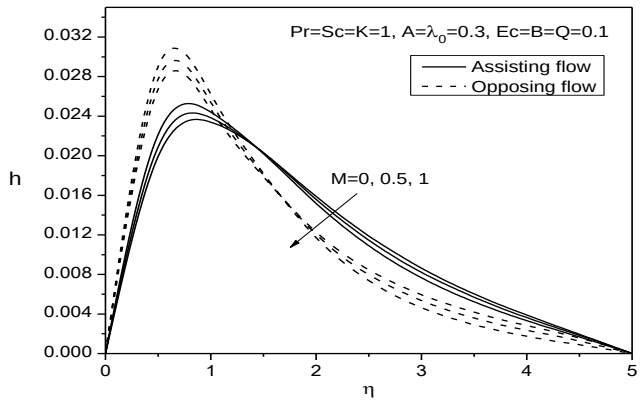

Fig.2 Angular velocity profiles for different values of M

ISSN: 2277-9655
(I2OR), Publication Impact Factor: 3.785

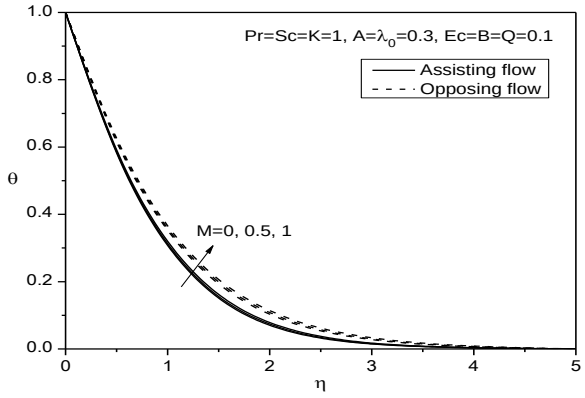

Fig.3 Temperature profiles for different values of M

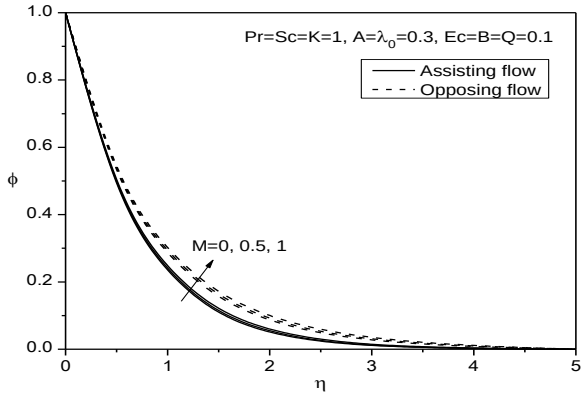

Fig.4 Concentration profiles for different values of M

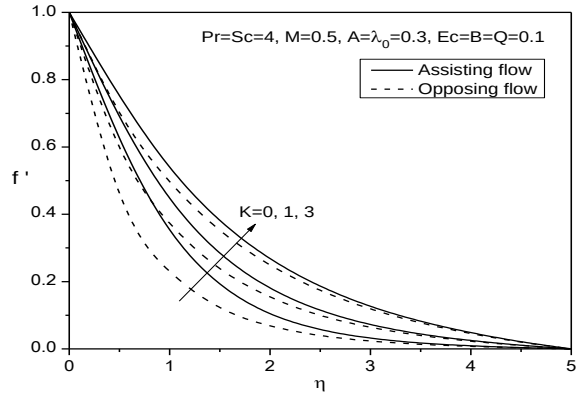

Fig.5 Velocity profiles for different values of K

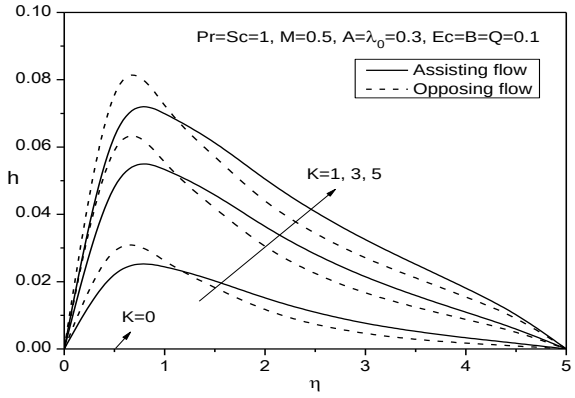

Fig.6 Angular velocity profiles for different values of K

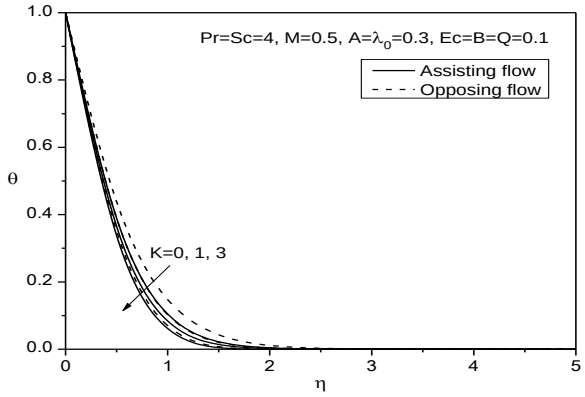

Fig.7 Temperature profiles for different values of K

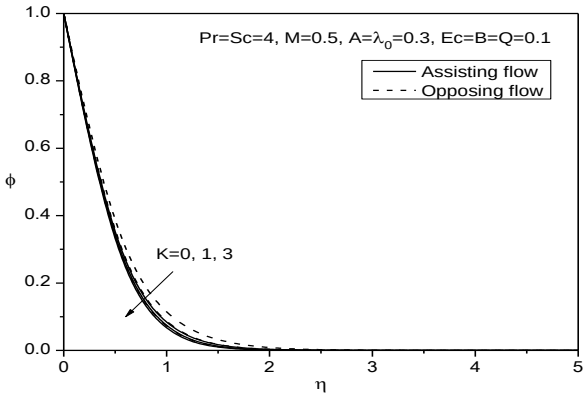

Fig.8 Concentration profiles for different values of K

ISSN: 2277-9655
(I2OR), Publication Impact Factor: 3.785

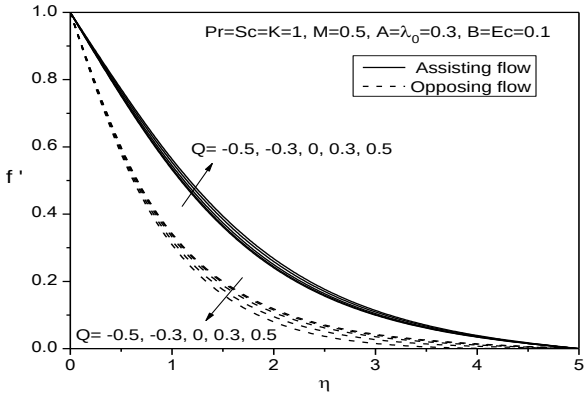

Fig.9 Velocity profiles for different values of Q

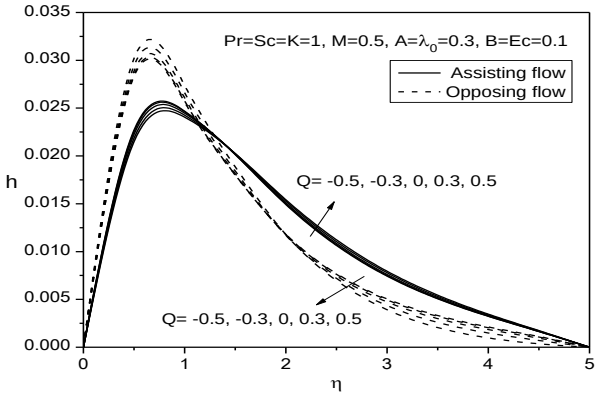

Fig.10 Angular velocity profiles for different values of Q

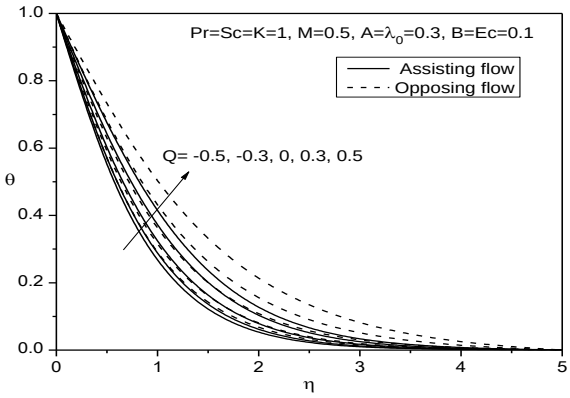

Fig.11 Temperature profiles for different values of Q

ISSN: 2277-9655
(I2OR), Publication Impact Factor: 3.785

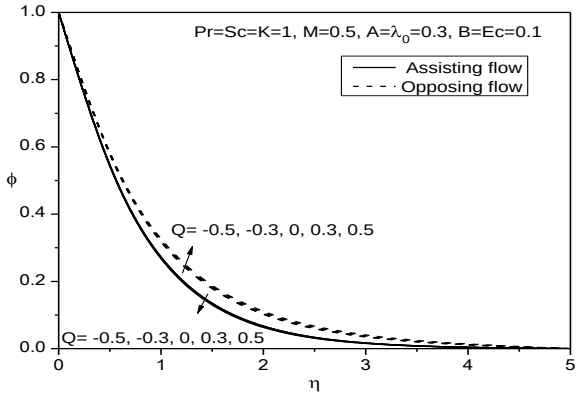

Fig.12 Concentration profiles for different values of Q

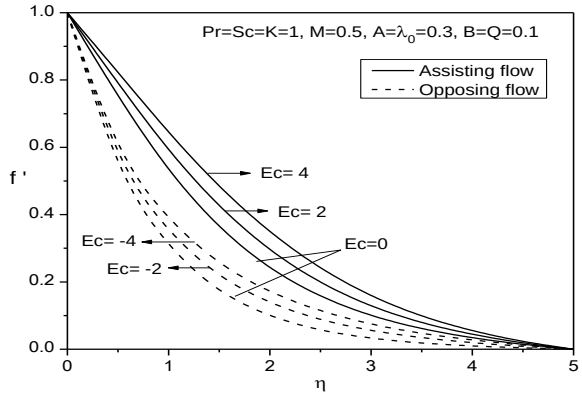

Fig.13 Velocity profiles for different values of Ec

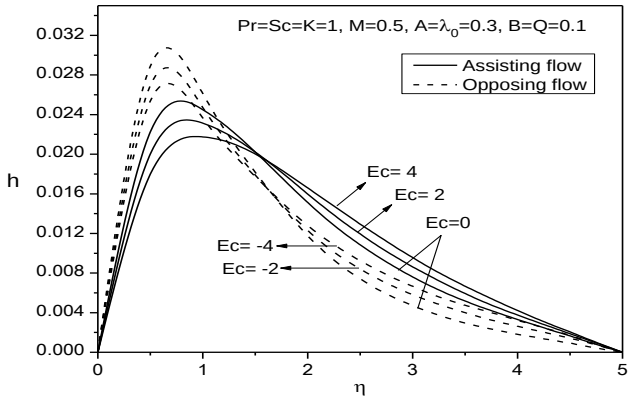

Fig.14 Angular velocity profiles for different values of Ec

ISSN: 2277-9655
(I2OR), Publication Impact Factor: 3.785

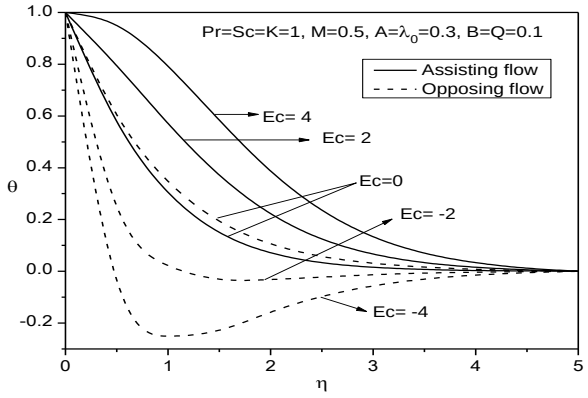

Fig.15 Temperature profiles for different values of Ec

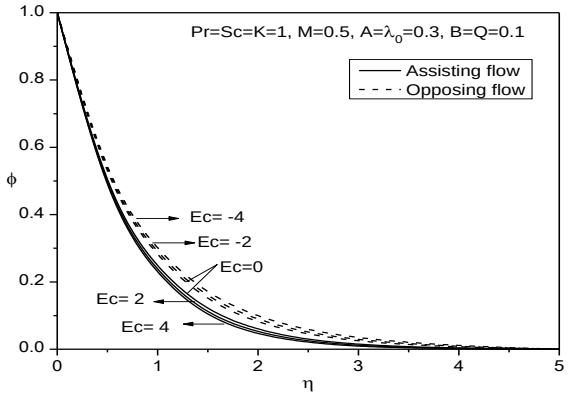

Fig.16 Concentration profiles for different values of Ec

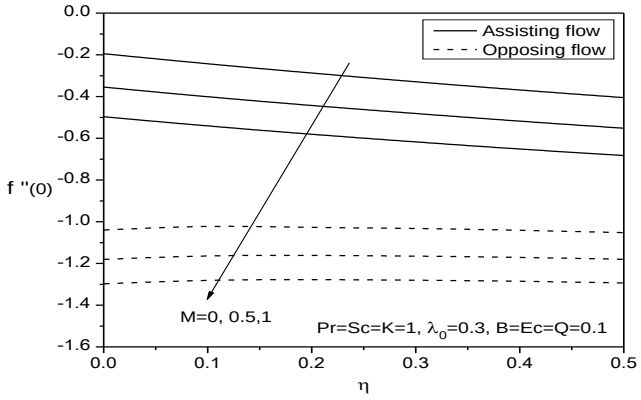

Fig.17 Profiles of Skin friction for different values of A and M

ISSN: 2277-9655
(I2OR), Publication Impact Factor: 3.785

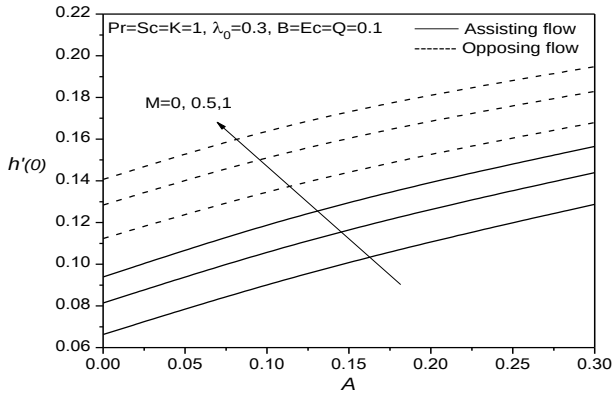

Fig.18 Profiles of Couple wall stress for different values of A and M

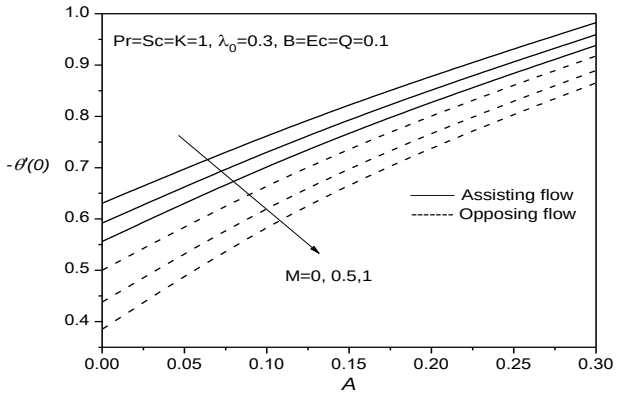

Fig.19 Profiles of Nusselt number for different values of A and M

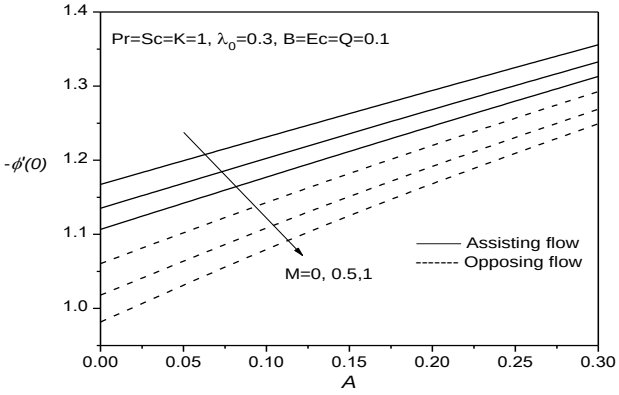

Fig.20 Profiles of Sherwood number for different values of A and M

ISSN: 2277-9655
(I2OR), Publication Impact Factor: 3.785

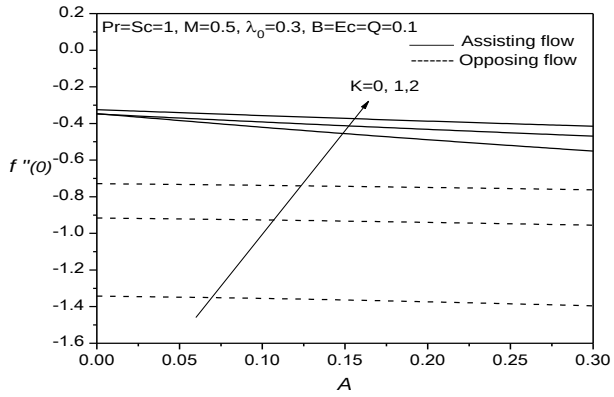

Fig.21 Profiles of Skin friction for different values of A and K

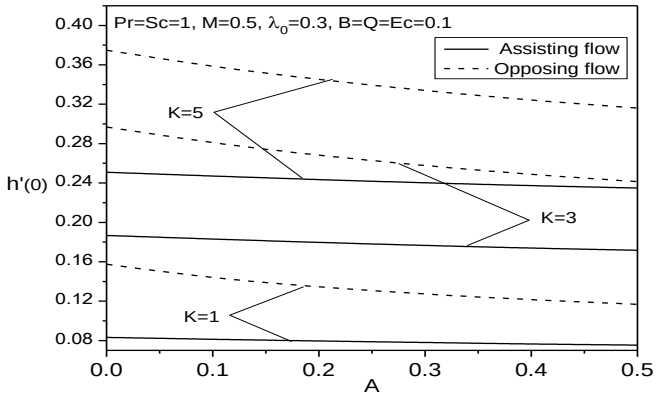

Fig.22 Profiles of couple wall stress for different values of A and K

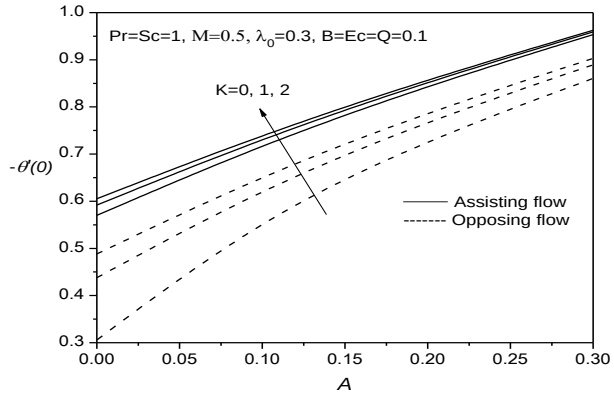

Fig.23 Profiles of Nusselt number for different values of A and K

ISSN: 2277-9655
(I2OR), Publication Impact Factor: 3.785

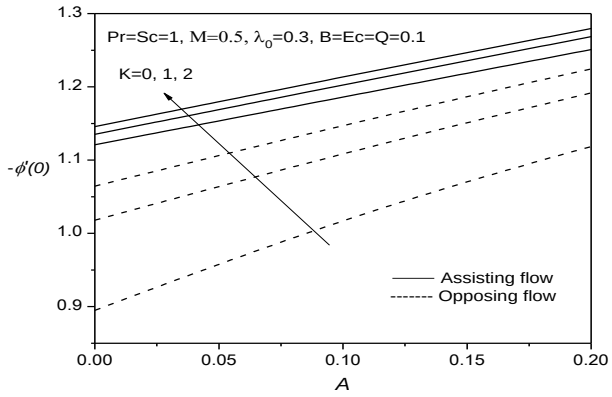

Fig.24 Profiles of Sherwood number for different values of A and K

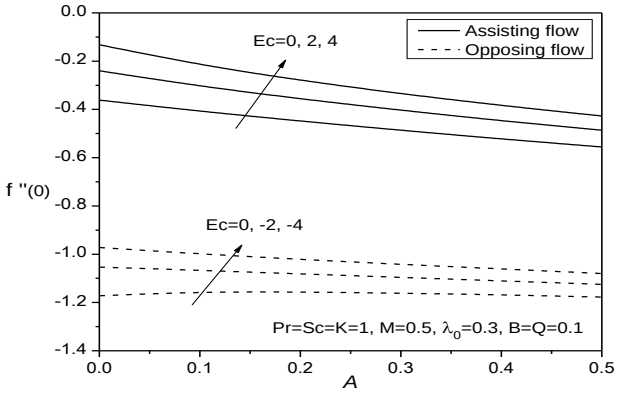

Fig.25 Profiles of skin-friction for different values of A and Ec

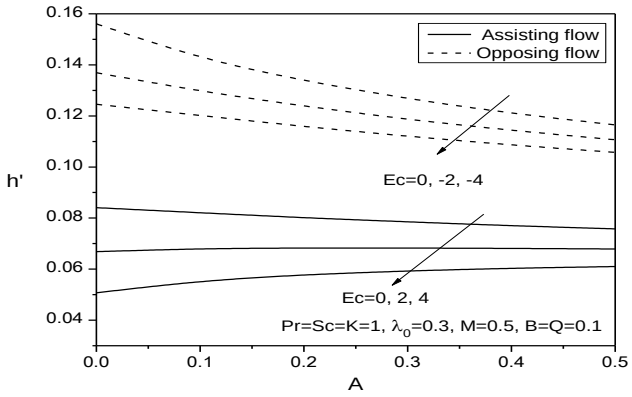

Fig.26 Profiles of couple wall stress for different values of A and Ec

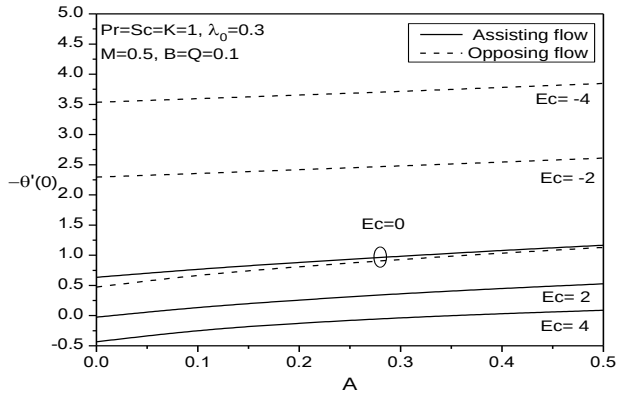

Fig.27 Profiles of Nusselt number for different values of A and Ec

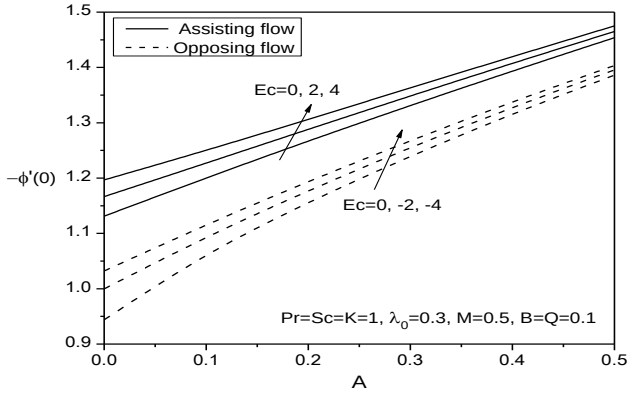

Fig.28 Profiles of Sherwood number for different values of A and Ec

Table 1 Comparison of $-\theta'(0)$ for those of Ishak et al. [31] for different values of A, λ and Pr when K=Q=Sc=M=0.

A	λ	Pr	$-\theta'(0)$	
			Present study	Ishak et al. [31]
0	0	0.72	0.80868	0.8086
0	0	1	1.0000	1.0000
0	0	3	1.92368	1.9237
0	0	10	3.70693	3.7207
0	0	100	12.293	12.2941
0	1	1	1.08728	1.0873
0	2	1	1.14233	1.1423
0	3	1	1.18528	1.1853
1	0	1	1.68195	1.6820
1	1	1	1.70383	1.7039
1	-0.5	10	3.86633	5.5585
1	0.5	10	3.89254	5.5690

REFERENCES

[1] Eringen, A.C., (1960), Theory of micropolar fluids, J. Math. Mech., Vol. 6, pp. 1-18.
[2] Eringen, A.C., (1972), Theory of thermomicropolar fluids, Math. Anal. Appl. J., Vol. 38, pp.481-496.
[3] Willson, A.J., (1970), Boundary-layer in micropolar liquids, Proc. Cambridge Philos. Soc., Vol. 67, pp.469–476.
[4] Bergholz, R.F., (1980), Natural convection of a heat generating fluid in a closed cavity, ASME J. Heat Transfer, Vol.102, pp.242–247.
[5] Chandra Shekar, B., Vasseur, P., Robillard, L., Nguyen, T.H., (1984), Natural convection in a heat generating fluid bounded by two horizontal concentric cylinders, Can. J. Chem. Eng., Vol. 62, pp.482–489.
[6] Peddiesen, J., McNitt, R.P., (1970), Boundary layer theory for micropolar fluids, Recent Adv. Eng., Vol. 5, pp.405–426.
[7] Lukaszewicz, G., (1999), Micropolar Fluids: Theory and Applications, Birkh a¨ user, Boston.
[8] Eringen, A.C., (2001), Microcontinuum Field Theories. II: Fluent Media, Springer, NewYork.
[9] Yih, K. A., (1999), Free convection effect on MHD coupled heat and mass transfer of a moving permeable vertical surface, Int. Commun. Heat Mass Transfer, Vol.26, pp.95-104.
[10] Anjali Devi, S.P. and Kandasamy, R., (2002), Effects of chemical reaction, heat and mass transfer on non-linear MHD laminar boundary layer flow over a wedge with suction or injection, Int. Commun. Heat Mass Transfer, Vol.29, pp.707-716.
[11] Alam, M.S., Rahman, M.M. and Maleque, A., (2005), Local similarity solutions for unsteady MHD free convection and mass transfer flow past an impulsively started vertical porous plate with Dufour and Soret effects, Int. J. Sci. Tech., Vol.10, pp.1-8.
[12] Xu, H. and Liao, S.J., (2005), Analytic solutions of magnetohydrodynamic flows of non-Newtonian fluids caused by an impulsively stretching plate, J. Non-Newton. Fluid Mech., Vol.159, pp.46-55.
[13] Abdelkhalek, M.M., (2009), Heat and Mass Transfer in MHD Free Convection from a Moving Permeable Vertical Surface by a Perturbation Technique, Commun. Nonlinear Sci. Numer. Simulat., Vol.14, pp.2091-2102.
[14] Soundalgekar, V.M., Patil, M.R. and Jahagirdar, M.D., (1981), MHD stokes problem for a vertical plate with variable temperature, Nuclear Engg Des, Vol.64, pp.39-42.
[15] Hasanpour, A., Farhadi, M., Sedighi, K., and Ashorynejad, H.R., (2010), Lattice Boltzmann Simulation for Magnetohydrodynamic Mixed Convective Flow in a Porous Medium, World App. Sci. J., Vol.11, pp.1124-1132.
[16] Kumar, A.G.V. and Verma, S.V.K., (2011), Thermal radiation and mass transfer effects on MHD flow past a vertical oscillating plate with variable temperature effects variable mass diffusion, Int. Journal of Engineering, Vol.3, pp.493-499.
[17] Arman Hasanpour, Mojtaba Parvizi Omran, Hamid Reza Ashorynejad, Davood Domairry Ganji and Naim Roshan, (2013), Investigation of Heat and Mass Transfer of MHD Flow over the Movable Permeable Plumb Surface Using HAM, World Applied Sciences Journal, Vol.21 (Special Issue of Applied Math), pp.07-16.
[18] Postelnicu, A., Grosan, T., and Pop, I., (2001), The effect of variable viscosity on forced convection over a horizontal flat plate in a porous medium with internal heat generation, Mechanics Research Communications, vol.28, no.3, pp. 331-337.
[19] Molla, M.M., Hossain, M.A., and Yao, L.S., (2004), Natural convection flow along a vertical wavy surface with uniform surface temperature in presence of heat generation/absorption, Int. J. Thermal Sci., Vol.43, pp.157-163.
[20] Samad, M.A., and Mohebujjaman, M., (2009), MHD heat and mass transfer free convection flow along a vertical stretching sheet in presence of magnetic field with heat generation, Research J. of Applied Sci., Eng. and Tech., Vol.1(3), pp.98-106.
[21] Bhaskar Reddy, N. and Bathaiah, D., Hydrodynamic channel flows under periodic rate of heat generation with Hall effects, Reg. J. of Energy Heat and Mass Transfer, 3, No.2, 97-112,1981.
[22] Alam, M. S., Rahman, M. M. and Samad, M. A., (2006), Numerical study of the combined free-forced convection and Mass transfer flow past a vertical porous plate in a porous medium with heat generation and thermal diffusion, Nonlinear Analysis: Modeling and Control,vol.11, no. 4, pp. 331-343.

[23] Mohammed Abdur Rahman, Alim, M. A. and Jahurul Islam, Md., (2013), Thermophoresis Effect on MHD Forced Convection on a Fluid over a Continuous Linear Stretching Sheet in Presence of Heat Generation and Power-Law Wall Temperature, Annals of Pure and Applied Mathematics, Vol. 4, No.2, pp.192-204
[24] Gebharat, B., (1962), Effects of viscous dissipation in natural convection, J. Fluid Mech., Vol. 14, pp.225-232.
[25] Gebharat, B., and Mollendorf, J., (1969), Viscous dissipation in external natural convection flows, J. Fluid. Mech.,Vol.38, pp.97-107.
[26] Neeraja, A. and Bhaskar Reddy, N., (2008), MHD unsteady free convection flow past a vertical porous plate with viscous dissipation, Ultra Science, Vol.20, No.1(M), pp.183-194.
[27] Mohamed Abd El-Aziz, (2013), Mixed convection flow of a micropolar fluid from an unsteady stretching surface with viscous dissipation, Journal of the Egyptian Mathematical Society, Vol. 21, pp.385–394.
[28] Andersson, H.I., Aarseth, J.B., Dandapat, B.S., (2000), Heat transfer in a liquid film on an unsteady stretching surface, Int. J. Heat Mass Transfer, Vol.43, pp.69-74.
[29] Jain, M.K., Iyengar, S.R.K. and Jain, R.K., (1985), Numerical Methods for Scientific and Engineering Computation, Wiley Eastern Ltd., New Delhi, India.
[30] Ishak, A., Nazar, R., and Pop, I., (2009), Boundary layer flow and heat transfer over an unsteady stretching vertical surface, Meccanica, Vol.44, pp.369–375.